Thermodynamic properties of illite, smectite and beidellite by calorimetric methods: Enthalpies of formation, heat capacities, entropies and Gibbs free energies of formation

Hélène Gailhanou, Philippe Blanc, J. Rogez, Georges Mikaelian, H. Kawaji, Juan Olives, V. Montouillout, Jean-Marc Greneche, Philippe Vieillard, Eric C. Gaucher, et al.

Thermodynamic properties of mixed-layers illite-smectite by calorimetric methods. Acquisition of the enthalpies of mixing of illite and smectite layers.

H. Gailhanou[1*], P. Blanc[1], J. Rogez[2], G. Mikaelian[2], H. Kawaji[3], J. Olives[4], V. Montouillout[5], J-M. Grenèche[6], P. Vieillard[7], E.C. Gaucher[1], C.I. Fialips[8], B. Made[8]

[1]BRGM, 3 av. C. Guillemin, BP6009, 45060 Orléans, France
[2]IM2NP, F.S.T. Saint-Jérôme, Case 251, Aix Marseille Université, 13397 Marseille Cedex 20, France
[3]Tokyo Institute of Technology, 4259 Nagatsuta-cho, Midori-ku, Yokohama, 226-8503 Japan
[4]CINaM-CNRS, Aix-Marseille Univ., Campus de Luminy, Case 913, 13288 Marseille Cedex 9, France
[5]CEMHTI-CNRS-UPR-3079, 1D av. de la Recherche Scientifique, 45071 Orléans, France
[6]IMMM-UMR-CNRS-6283, Le Mans Université, 72085 Le Mans cedex, France
[7]CNRS-IC2MP-UMR-7285 Hydrasa, 5 av. Albert Turpain, 86073 POITIERS-Cedex, France
[8]ANDRA, 92298 Châtenay-Malabry, France.

Corresponding author:
Hélène GAILHANOU
BRGM, 3 av. Claude Guillemin BP6009
45060 Orléans, France.
*E-mail: h.gailhanou@brgm.fr

Abstract --- The stability of illite-smectite interstratified with respect to discrete illite and smectite minerals was investigated by measuring thermodynamic properties. The standard thermodynamic properties of the illite-smectite ISCz-1 (G, H, S, Cp, V) were determined between 298.15K and 375K by using calorimetric methods. Moreover, the enthalpies of mixing between illite and smectite layers were measured at 298.15K by acid solution calorimetry from a complete serie of illite-smectite interstratified minerals (Shinzan area, Japan). The measured values were slightly negative, with a minimum value at -3.7 $kJ.mol^{-1}$, and contribute to the stability of the mixed-layer with respect to a mechanical mixture of illite and smectite. Besides, the model from Blanc et al. (2015) was implemented to estimate the thermodynamic properties of the interstratified illite-smectite ISCz-1 mineral. The predicted values were consistent with the experimental ones. However, the estimates were slightly improved by considering the thermodynamic properties of the mixture of illite and smectite components and then adding the terms of energies of mixing. This could be confirm by setting up the stability domains of ISCz-1 and the corresponding illite and smectite end-members, according to Meunier and Velde (1989) determination of the smectite to illite reaction pathways.

Key words: illite, smectite, enthalpies, heat capacities, entropies, Gibbs free energies, calorimetry, enthalpies of mixing

Running title: Thermodynamic properties of illite-smectite by calorimetry

1. INTRODUCTION

Illite/smectite mixed layer clay minerals (I/S) are widely present in natural environment and occur in various contexts, notably during diagenetic processes in sedimentary basins (Perry and Hower, 1970; Hower et al., 1976, among others), or resulting from the hydrothermal alteration of volcanic or plutonic rocks (Steiner, 1968; McDowell and Elders, 1980; Inoue and Utada., 1983, among others). Understanding the processes associated with the transformation of smectite into illite/smectite and consequences on the mechanical and the geochemical behaviour of the clayey formation is of great importance in some major applications fields, such as oil exploration or nuclear waste disposal. For instance, this transformation is an indicator of possible oil reserves for a given reservoir. It was and is still widely used as a geothermometer for the early diagenesis stage (possibly combined with other tools like the Na/K or Si geothermometer or stable isotope analyses) in order to assess the maturity, in terms of P-T-X reaction pathway, of a given reservoir (Velde and Vasseur, 1992). In addition, the smectite-to-illite conversion may generate overpressures in sedimentary basins due to the dehydration of smectite and the precipitation of secondary minerals (Powers, 1967; Colton-Bratley, 1987; Osborne and Swarbrick, 1997) that can be problematic for the functioning of oil wells. Besides, according to Gaucher and Blanc (2006) review, the smectite transformation to illite-smectite and then illite could be possibly expected at cement/clay interfaces, after long period of reaction times, within the framework of deep disposal. Alkaline disturbance will generate mineralogical transformations at the cement/clay interface, in particular of bentonite, implying a decrease of smectite content. This latter will affect the swelling properties and the retention capacities of clayey barriers. Such reactions have to be integrated in the geochemical calculations used for performance assessment.

The thermodynamic stability of illite/smectite remains an unsolved issue. Numerous studies based on mineralogical characterization of clays in natural systems (Inoue et al., 2005; Ylagan et al., 2000; Murakami et al., 2005; Claret et al., 2004; McCarty et al., 2008; Lanson et al., 2009, among others) and on laboratory experiments (Ferrage et al., 2011; Yates and Rosenberg, 1996, 1997; Rosenberg et al., 1990; Whitney and Northrop, 1988; Whitney and Velde, 1993, among others) were performed in order to better understand the

reaction mechanisms of the smectite illitization during hydrothermal alteration and diagenetic processes. Several authors (Whitney and Northrop, 1988; Whitney and Velde, 1993; Rosenberg et al., 1990; Yates and Rosenberg, 1996; Ferrage et al., 2011 and references therein) showed the coexistence of several phases (smectite, illite and one or more intermediate illite/smectite phases) during the transformation of smectite to illite. Collecting the chemical analyses of natural I/S samples, Meunier and Velde (1989) have described the interstratified minerals by a ternary solid-solution model with one illite and two montmorillonite end-members. Based on this approach, Blanc et al. (1997) developed a thermodynamic model allowing the calculation of the energies of mixing of illite and smectite layers depending on the degree of ordering of the stacking sequences. The resulting Gibbs free energies of mixing are then slightly negative, suggesting the stability of illite-smectite mixed-layers with respect to the mechanical mixture of pure illite and smectite layers.

The present work focuses on the measurement of thermodynamic properties for I/S minerals with two main objectives:

- to acquire a complete set of thermodynamic properties (G, H, S, Cp) for an illite-smectite mineral (ISCz-1), based on calorimetric methods (Gailhanou et al., 2012, 2013), which could be used to supply the thermodynamic databases (e.g., ThermoChimie (Giffaut et al., 2014) and Thermoddem (Blanc et al., 2012)) for geochemical modelling calculations. Until now, the lack of thermodynamic data for illite/smectite mixed layers is a limitation to properly model the smectite-to-illite conversion;
- to acquire the enthalpies of mixing of illite-smectite layers for a series of interstratified illite-smectite (hydrothermal alteration minerals, coming from Shinzan Area; Inoue and Utada, 1983, Inoue et al., 1987).

Besides, the present work allows checking the reliability of the predictive model from Blanc et al. (2015) for the thermodynamic properties of interstratified illite-smectite. Based on the properties measured here, the influence of the thermodynamic parameters of mixing can be discussed, including the configurational entropy associated with cationic disordering in crystallographic sites of clay minerals and specific interactions between smectite and illite layers, within the I/S stacking sequence.

2. MATERIALS AND METHODS

2.1. Clay samples

The ISCz-1 sample is a mixed-layer illite-smectite, originating from Slovakia. It was provided by the Source Clays Repository of the Clay Minerals Society (Chipera and Bish, 2001).

After sieving the ISCz-1 sample at a size < 20 µm, the < 2 µm fraction was separated by centrifugation. This latter was then twice dispersed in $CaCl_2$ 0.5 M solution during 24h and centrifuged. Therefore, the sample was washed with a $CaCl_2$ 0.001 M solution, by using dialysis bag for 3 days. In the present study, Ca^{2+} was preferred to Na^+ for the saturation of the smectitic interlayers, to facilitate the washing of the clay sample by avoiding osmotic swelling of smectite. Eventually, the sample was dried at 40°C then 60°C for several days. In the following, the sample referenced ISCz-1 designates this treated sample.

A series of fourteen illite-smectite mixed-layers samples coming from the Shinzan area, northeast Japan, has also been used for this study. This series, well described in literature (Inoue et al., 1987; Inoue and Utada, 1983), is noticeable as it consists in a complete mixed-layers series with chemical compositions varying from montmorillonite to illite end-members. The series results from the hydrothermal alteration of dioctahedral micas/smectites. The continuous conversion of smectite into illite has been described in Inoue et al. (1987). The main transformation mechanism suggested by the authors was based on the dissolution of smectite and the crystallization of illite. A solid-state transformation mechanism was also shown from HRTEM observations (Amouric and Olives, 1991; Olives et al., 2000).

2.2. Analysis and characterization of the samples

2.2.1. ISCz-1 sample

Chemical analyses for Si, Al, Ti, Fe(total), Mn, Ca, Mg, K, Na and P were performed by X-ray fluorescence spectrometry. The results of the analysis are presented in Table 1; the relative uncertainties are estimated at

±2 %. The amounts of total carbon and total sulfur were determined by infra-red spectroscopy after burning the samples at 900 °C in an oxygen atmosphere. The amount of Fe^{2+} was determined by ^{57}Fe Mössbauer spectrometry, as described further in the text.

The chemical composition of the ISCz-1 sample (Ca-saturated) differs slightly from the previous Na-saturated ISCz-1 sample used for heat capacity measurements in Gailhanou et al. (2007) (Table 1). Both samples were supplied by the Clay Minerals Society with several years of intervals. The following study of the thermodynamic properties of the present ISCz-1 sample is complementary to the previous work from Gailhanou et al. (2007).

Table 1 Chemical analyses of the sample ISCz-1 (< 2µm clay fraction). (a) X-ray fluorescence; (b) ^{57}Fe Mössbauer spectrometry; (c) weight loss by heating up to 1000°C; (d) infra-red spectroscopy.

	ISCz-1 (this study) wt.%	Na-sat. ISCz-1 (Gailhanou et al., 2007) wt.%	Analytical technique
SiO_2	53.8	52.6	(a)
Al_2O_3	24.4	26.7	(a)
CaO	1.1	< 0.1	(a)
Fe_2O_3	1.39	0.97	(a), (b)
FeO	0.17	0.30	(b)
K_2O	5.07	5.96	(a)
MgO	2.2	2.1	(a)
Na_2O	< 0.2	1.0	(a)
TiO_2	0.13	0.09	(a)
P_2O_5	< 0.05	0.13	(a)
Loss on ignition	11.9	10.0	(c)
C total	0.07	0.04	(d)
S total	< 0.01	0.06	(d)
Total	100.25	99.95	

The cationic exchange capacity (CEC) of the sample was measured after saturating the sample with a chloride cobalt hexammine solution, according to the method described in Gaucher et al. (2009). The total CEC was measured by colorimetry and the exchangeable cations (Na^+, Ca^{2+}, K^+, Mg^{2+}) were analyzed by ionic chromatography. The results are provided in Table 2. The obtained CEC value is consistent with the one measured for the ISCz-1 sample in Gailhanou et al. (2007), at 39.0 meq/100 g.

Table 2. CEC measured for ISCz-1 sample (< 2 µm clay fraction), in meq/100 g of dry sample.

Sample	Na	Ca	Mg	K	Sum of exch. Cations	CEC (colorimetry)
ISCz-1	0.4	39.7	< 0.5	3.8	43.9	44.1

Moreover, XRD analyses were carried out on the ISCz-1 sample, on powder and on oriented deposit, using the method described in Gailhanou et al. (2007). For the powder sample, both an identification of the nature of impurities and a semi-quantification were performed by using Modpattern (Guyonnet et al., 2009) with an internal corundum standard (Figure 1). In the present case, only rough estimates of the proportions of the impurities could be obtained by modelling, due to the lack of a reference pattern for Ca-saturated illite-smectite.

Moreover, the modelling of the XRD pattern on the glycolated, oriented deposit was performed by using the Arquant code (Blanc et al., 2007) and allowed the identification and the quantification of a small amount of kaolinite. Finally, the amounts of impurities in the purified sample estimated by XRD modeling are 4.2, 3.8 and 0.45 wt.% of quartz, K-feldspar and kaolinite, respectively. Moreover, resulting from the modelling of the XRD pattern on the glycolated deposit and in agreement with Chipera and Bish (2001) results, the interstratified ISCz-1 was ordered with a degree of interstratification ordering R = 1 (Reichweite index) and the illite layers content was estimated at 70 %.

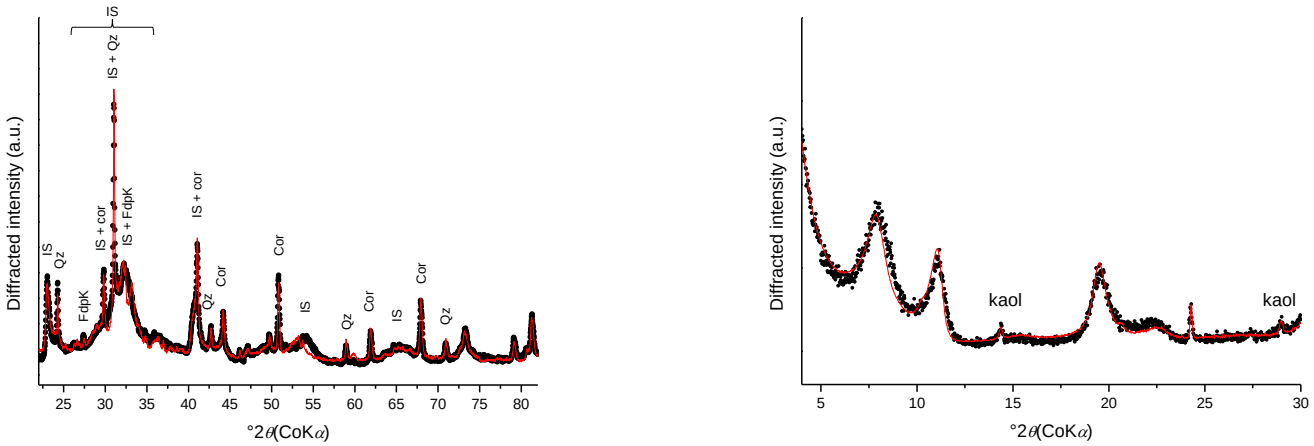

(a) (b)

Figure 1. Modelled XRD patterns obtained for ISCz-1 sample (< 2 µm, Ca-saturated) on (a) powder sample and (b) glycolated oriented deposit. IS = mixed-layer ISCz-1; Qtz = quartz; Cor = corundum (internal standard, 9.19 wt.%); FdpK = K-feldspar; Kaol = Kaolinite (in black, experimental; in red, modelling).

Besides, some investigations were performed by using ^{29}Si and ^{27}Al NMR in order to complete the characterization of the silicates and aluminosilicates impurities. A ^{29}Si NMR spectrum was acquired with a Bruker Advance 300 MHz (B0 = 7.0 T) spectrometer, operating at 79.5 MHz frequency for ^{29}Si (Figure 2(a)). It revealed notably, in addition to illite-smectite component (between -80 and -100 ppm), the presence of quartz (-107.52 ppm) and the absence of other silica impurity (cristobalite or amorphous silica, notably). The amount of quartz was estimated to 5.4 wt.% in the ISCz-1 sample. This result is in good agreement with the XRD estimate at 4.2 wt.%.

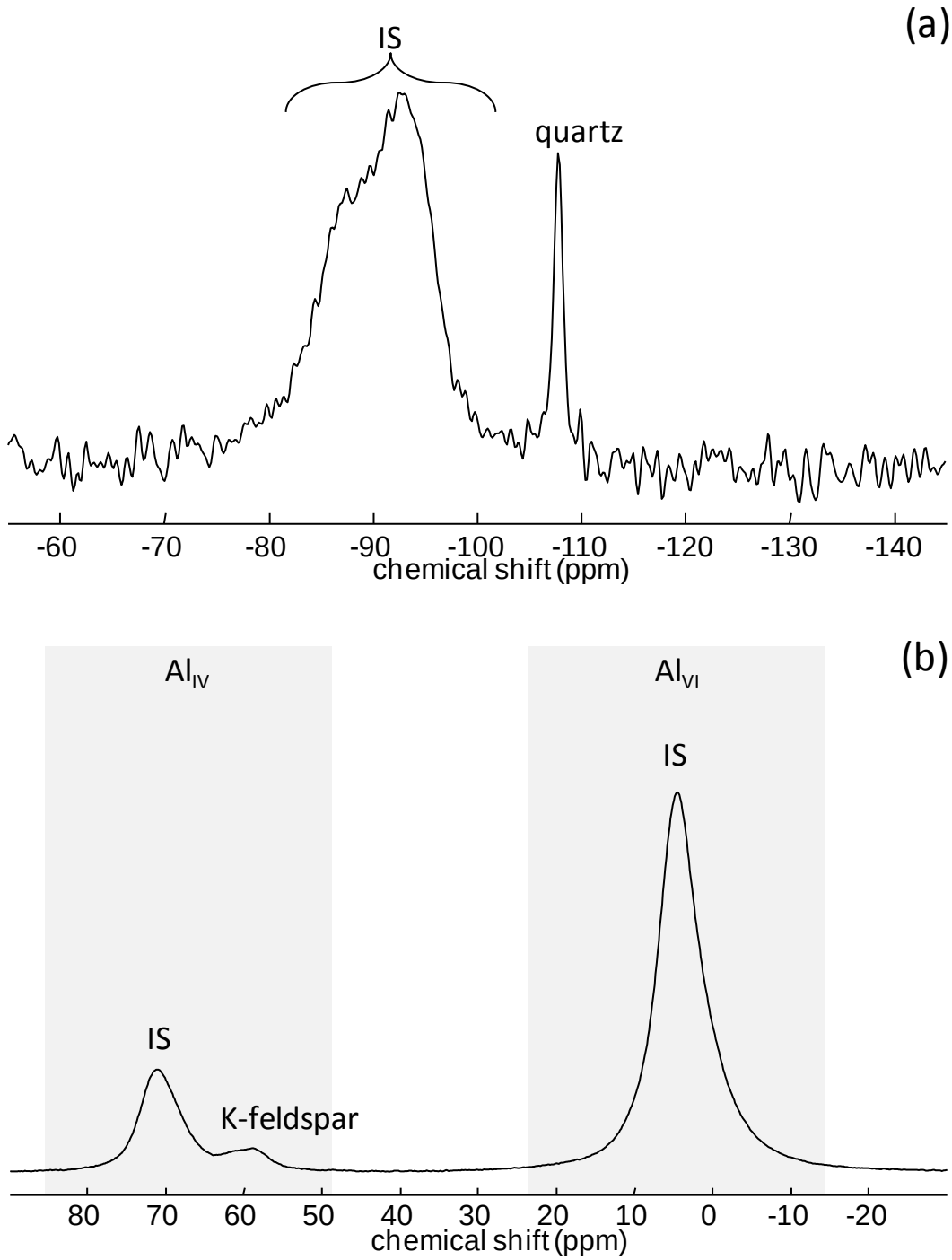

177

178 Figure 2. Identification and quantification of impurities in ISCz-1 sample (< 2 µm clay fraction) by NMR: (a) ^{29}Si and (b)

179 ^{27}Al NMR spectra.

180

181 For its part, the ^{27}Al NMR spectrum (Figure 2 (b)) acquired with a Bruker Advance 750 MHz spectrometer

182 (B_0 = 17.7 T, ν_{RF}(^{27}Al) = 195.5 MHz) exhibits three main signals for one six-fold coordinated aluminum

(δ_{CG} = 4.6 ppm) and two four-fold coordinated aluminum (δ_{CG} = 59.4 and 71.1 ppm). Both δ_{CG} = 4.6 and 71.1 ppm sites are commonly attributed to Al^{VI} and Al^{IV} in illite-smectite (Cuadros and Linares, 1996; Garg and Skibsted, 2016), while the signal at δ_{CG} = 59.4 ppm is compatible with Al^{IV} in K-feldspar, detected by XRD (Cuadros and Linares, 1996). The spectrum was modeled using the Dmfit software (Massiot et al., 2002). The component at δ_{CG} = 59.4 ppm corresponds to 2.9 at % of the aluminum of the sample. The resulting proportion of K-feldspar impurity in the ISCz-1 sample was then estimated to 3.8 wt.%, in agreement with the value obtained by XRD modeling.

The proportions of ferric and ferrous ions in the clay mineral and, if present, the amounts of ferrous or ferric impurities can be determined by ^{57}Fe Mössbauer spectrometry. These analyses were performed using a conventional constant acceleration Mossbauer spectrometer, in transmission geometry, equipped with a ^{57}Co(Rh) source. The isomer shift values were corrected according to the calibration of the velocity scale made from α-Fe at 300 K. The amount of Fe in the sample was about 5 mg/cm^2. The spectra obtained at 300 and 77 K were fitted using a discrete number of independent quadrupolar doublets and magnetic sextets composed of lorentzian lines where the line width at half-height Γ (mm.s^{-1}), the isomer shift δ (mm.s^{-1}) and the quadrupole splitting ΔE_Q (mm.s^{-1}) were refined using a least-square fitting procedure.

The ^{57}Fe Mössbauer spectra for the ISCz-1 sample (< 2 µm) are displayed in Figure 3. The 300K spectrum (inset Fig. 3) exhibits a quadrupolar broadened asymmetrical feature and a single line which can be described by means of two components clearly attributed to ferric and ferrous species. But one can see that the baseline remains distorted (as confirmed by a spectrum obtained at 12 mm/s, not shown here): this feature results from the presence of superparamagnetic Fe species, i.e. the presence of ultra-fine Fe-containing grains. Consequently, the hyperfine structure was investigated at 77K to get blocked magnetic states of some Fe species, as confirmed in Fig.3. The description requires unambiguously several magnetic sextets and quadrupolar doublets but a single broadened line was added to better describe the baseline. The refined values of Mössbauer parameters extracted from spectral modeling are listed in Table 3. The proportion of Fe in the clay mineral was estimated to 42 at.% of the total Fe content and the ratio $Fe^{3+}/(Fe^{2+}$ +

Fe^{3+}) to 72 % (Table 5). It is important to note the good agreement between the Fe^{2+} contents estimated at 300K and 77K, assuming that the proportions are proportional to the relative absorption areas, i.e. assuming the same values of the Lamb-Mössbauer recoilless factors. The modeling allowed to distinguish three magnetic phases, goethite (α-$Fe^{3+}O(OH)$) as fine grains (magnetic sextets) and ultra-fine superparamagnetic grains (single line) and probably bernalite (ideally $Fe^{3+}(OH)_3$, McCammon et al., 1995) or bernalite/hematite mixture.

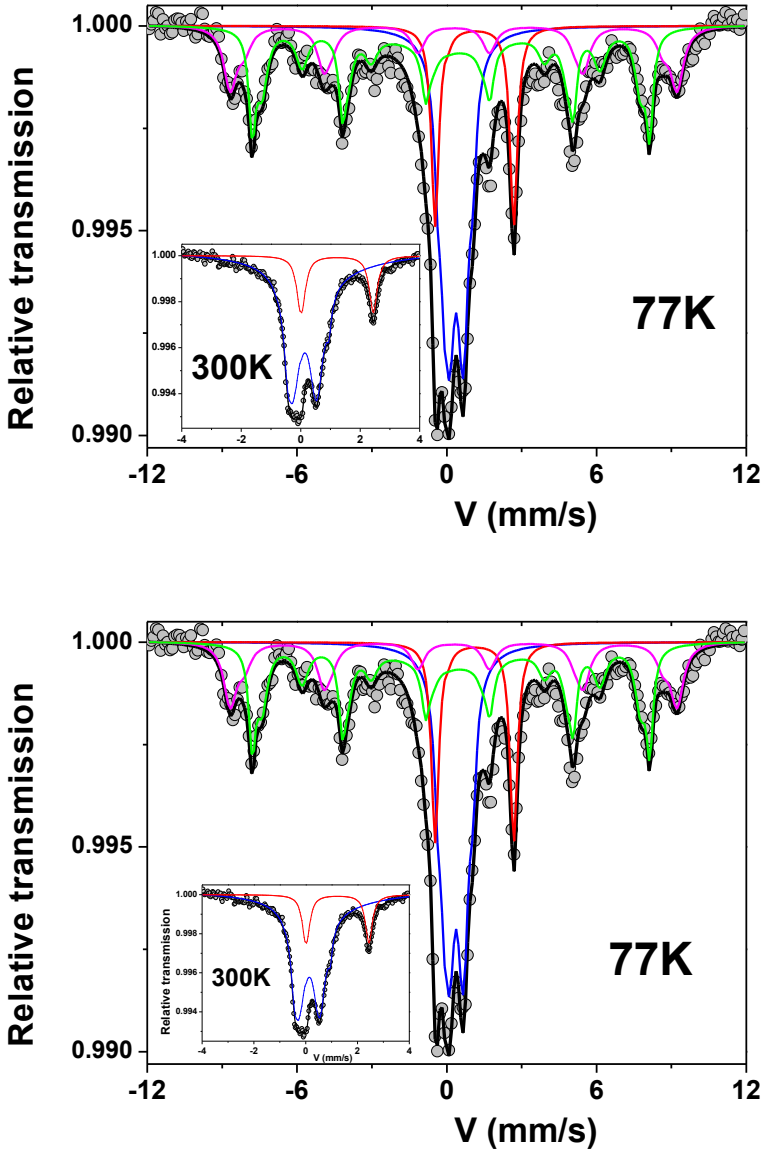

Figure 3. ^{57}Fe Mössbauer spectra for sample ISCz-1 (< 2 µm clay fraction). The 77K spectrum and its decomposition into 4 components: in red, for Fe^{2+} in clay; in dark blue, for Fe^{3+} in clay; in green, magnetic component for Fe^{3+} in

goethite; in pink, magnetic component for Fe^{3+} in bernalite. Inset represents the 300K spectrum with blue and red components attributed to ferric and ferrous species, respectively (see text).

Table 3. ^{57}Fe Mössbauer parameters at 77 K for the ISCz-1 sample (< 2 µm clay fraction)

Mineral	I.S. (mm/s)	$2\varepsilon/\Delta E_Q$ (mm/s)	B_{hf} (T)	%	attributions
	± 0.02	± 0.01		± 2	
Illite-smectite	0.47	0.57		27	Fe^{3+} associated with clay minerals (structural and/or sorbed ions)
	0.42	1.32		4	Fe^{3+} associated with clay minerals
Illite-smectite	1.30	3.06		12	Fe^{2+} associated with clay minerals
Goethite	0.46 0.47 0.47	-0.27 -0.27 -0.27	49.2 46.7 36.8	28	Fe^{3+} in goethite
Bernalite	0.40 0.40	0.00 0.00	51.8 55.3	17	Fe^{3+} in bernalite
Goethite (ultra-fine grains)	0.46	0.00		12	Fe^{3+} in goethite

I.S. = Isomer shift value relative to that of the α-Fe at 300 K; 2ε: quadrupolar shift; ΔE_Q = quadrupolar splitting value; B_{hf} = magnetic field; % = ratio of each component.
The 2σ standard errors for I.S., 2ε, ΔE_Q, B_{hf} and % are, respectively, ± 0.02, ± 0.02, ± 0.01, ± 0.5 and ± 2.

Thus, from these results and considering the total amount of Fe_2O_3 in the sample (Table 1), the amounts of goethite and bernalite were estimated to 0.70 wt.% and 0.36 wt.%, respectively.

From the preceding results, the final amounts of impurities were calculated and are reported in Table 4. The mean structural formula of illite-smectite was eventually calculated (Table 4) by subtracting the contributions of impurities, obtained at ambient R.H., to the global chemical analyses from Table 1.

Table 4. Amounts of impurities in the ISCz-1 sample, mean structural formula and molar mass of illite-smectite.

Impurity	Amounts at ambient R.H. (wt.%)	Amounts in dry sample (wt.%)	Analytical mean
Kaolinite	0.45	0.49	XRD
Quartz	5.40	5.85	^{29}Si NMR
K-feldspar (orthoclase)	3.80	4.12	^{27}Al NMR
goethite	0.70	0.76	^{57}Fe Mössbauer
bernalite	0.36	0.39	^{57}Fe Mössbauer
Sample	Mean structural formula		Molar mass ($g.mol^{-1}$)
ISCz-1 (this work)	$(Ca_{0.092}K_{0.440})(Si_{3.562}Al_{0.438})(Al_{1.721}Mg_{0.255}Fe^{3+}_{0.029}Fe^{2+}_{0.011}Ti_{0.008})O_{10}(OH)_2$		382.01
ISCz-1 (Gailhanou, 2007)	$(Na_{0.134}K_{0.530})(Si_{3.565}Al_{0.435})(Al_{1.717}Mg_{0.218}Fe^{3+}_{0.050}Fe^{2+}_{0.017})O_{10}(OH)_2$		385.04

Finally, the mineralogical and chemical compositions of the present ISCz-1 sample were compared to those obtained for the previous Na-saturated ISCz-1 sample, which had been used for heat capacity measurements in Gailhanou et al. (2007). Both samples were supplied by the Clay Minerals Society with several years of intervals. The amounts of impurities are significantly higher in the present ISCz-1 sample than in the previous one, which contained about 0.75 wt.% of quartz and 1.5 wt.% of kaolinite. Moreover, the mean structural formula of the Ca-saturated ISCz-1 sample (this study) exhibits a slightly lower total layer charge (0.62 eq./$O_{10}(OH)_2$) compared with the one previously obtained for the Na-saturated ISCz-1 sample, at 0.66 eq./$O_{10}(OH)_2$. The decrease of the layer charge is probably correlated to the increase of the total CEC, respectively 0.44 and 0.39 $eq.kg^{-1}$, for the present Ca-saturated ISCz-1 sample and the previous Na-saturated ISCz-1 sample, both indicating an amount of smectite layers slightly higher in the present case than for the sample analyzed previously.

2.2.2. Illite-smectite series from the Shinzan Area

The illite/smectite samples covers all the range of compositions from 0 % to 100 % of smectite (Table 5) as determined by X-ray diffraction from ethylene-glycol solvated samples (Inoue et al., 1987). According to these authors, the samples containing more than 50 % of smectite layers were randomly interstratified (Reichweite index R = 0), while the degrees of interstratification ordering increased progressively to R = 1, R = 2 and R ≥ 3 with increasing illite contents.

The chemical compositions of all the studied samples were determined by atomic absorption spectroscopy (Perbost et al., 2002). The mean structural formulae for the illite/smectite samples are given in Table 6.

Table 5. Illite/smectite interstratified minerals from the Shinzan hydrothermal alteration area in Japan.

Sample	Drill Hole	Depth (m)	% smectite layers
A (smectite)	Ws-2	183,5	100 % (R = 0)
B	Ws-4	329,5	85 % (R = 0)
C	Ws-4	383,0	73 % (R = 0)
D	Ws-2	377,8	70 % (R = 0)
E	Ws-2	407,4	68 % (R = 0)
F	Ws-4	392,8	50 % (R = 0)
G	Ws-2	423,2	40 % (R = 1)
H	Ws-10	199,9	35 % (R = 1)
I	Ws-4	440,6	30 % (R = 1)
J	Ws-5	240,1	20 % (R = 2)
K	Ws-7	123,6	15 % (R ≥ 3)
L	Ws-7	115,5	15 % (R ≥ 3)

M	Ws-7	197,0	5 % (R ≥ 3)
N (illite)	Ws-8	420,9	0 %

Table 6. Mean structural formulae of illite/smectite mixed-layers from the Shinzan area, on the basis of 12 oxygen atoms.

	A	B	C	D	E	F	G	H	I	J	K	L	M	N
Si	3.886	3.822	3.786	3.714	3.692	3.728	3.586	3.524	3.560	3.483	3.542	3.473	3.397	3.329
Al	1.685	1.658	1.722	1.847	1.908	1.738	2.079	2.059	2.036	2.268	2.101	2.214	2.316	2.401
Fe^{3+}	0.124	0.116	0.096	0.086	0.069	0.130	0.078	0.070	0.096	0.033	0.017	0.029	0.033	0.065
Fe^{2+}	0.020	0.035	0.025	0.025	0.042	0.037	0.019	0.038	0.028	0.040	0.017	0.023	0.029	0.055
Mg	0.314	0.397	0.390	0.340	0.304	0.388	0.258	0.314	0.301	0.190	0.332	0.264	0.231	0.171
Ti	0.012	0.006	0.009	0.020	0.011	0.005	0.003	0.045	0.009	0.008	0.015	0.018	0.003	0.005
Mn	0.000	0.000	0.000	0.000	0.000	0.001	0.000	0.000	0.000	0.001	0.002	0.003	0.007	0.001
Ca	0.072	0.063	0.049	0.022	0.025	0.038	0.029	0.027	0.026	0.023	0.013	0.009	0.022	0.001
Na	0.162	0.223	0.211	0.258	0.226	0.152	0.208	0.101	0.103	0.004	0.004	0.004	0.005	0.011
K	0.008	0.148	0.222	0.235	0.292	0.388	0.353	0.481	0.516	0.621	0.686	0.702	0.769	0.802

N.B. : Fe^{3+} and Ti were assumed to be in the octahedral sheets.

A statistical analysis of the chemical compositions of the I/S minerals was performed using the Principal Component Analysis method (XLSTAT©). The main trend for the chemical dispersion is described by the eigenvector $\mathbf{F_1}$ and corresponds to the substitution Si → KAl occurring during the transformation of montmorillonite to illite (Figure 4). A second trend, less important, seems to emerge along the $\mathbf{F_2}$ axis. Regarding the composition of the eigenvector $\mathbf{F_2}$, it represents the chemical dispersions for the elements Si, Mg and Al and shows a correlation between Si and Mg, whereas these latter are anti-correlated with Al. Then, the dispersion of compositions along $\mathbf{F_2}$ axis is probably associated with the Tschermak substitution $Al^{IV}Al^{VI}$ → $Si^{IV}Mg$, corresponding to muscovite → celadonite. Finally, the main chemical dispersion occurs along the montmorillonite N – illite A axis, as expected. Nevertheless, because some compositions deviate from this axis, it is also necessary to take into account a supplementary dimension, along the $\mathbf{F_2}$ axis, in order to describe all the compositions of the I/S minerals. In the following, we propose to describe the compositions of these illite-smectite series by a ternary solid-solution, composed of illite N, montmorillonite A and interstratified F end-members. The interstratified F was selected as it exhibits the stronger celadonite-type component along $\mathbf{F_2}$ (Figure 4).

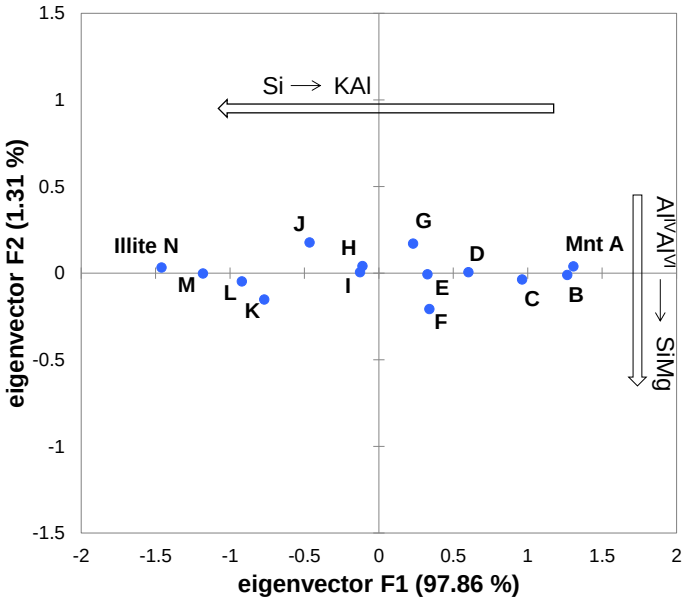

Figure 4. Statistical treatment by PCA of the 14 compositions of the I/S from Shinzan area. The chemical trends shown by arrows were depicted from the components of the main eigenvectors F_1 and F_2 (see text). Mnt A = Montmorillonite A.

2.2.3. Hydration state of samples for calorimetric measurements

The calorimetric measurements were performed on dehydrated ISCz-1 sample. The dehydrated state was obtained by heating the sample at 150°C for 20 hours. The sample was then stored in a glove box under dry Ar atmosphere (H_2O < 4 ppm).

For the interstratified samples from the Shinzan hydrothermal area, the enthalpies of dissolution were acquired by Perbost et al. (2002). The samples were stored at room relative humidity before the measurements. Their hydration states were not determined. Nevertheless, slight variations in the relative humidities, and therefore in the amounts of water adsorbed for a given sample, were not expected to affect significantly the enthalpy of dissolution of the sample, because the contribution of the enthalpy of dilution is negligible compared to the total measured enthalpy of dissolution and its associated uncertainty.

2.3. Calorimetric methods

2.3.1. Heat capacity measurements

For the dehydrated ISCz-1 sample, the heat capacities were measured by heat-pulse calorimetry between 2 and 330 K, using a commercial apparatus (PPMS model 6000, Quantum Design Inc.; Dachs and Bertoldi

(2005)). Measurements were performed twice in the temperature range, by cooling the sample from 50 K to 2 K and heating from 50 K to 330 K, respectively. They were carried out on two pressed pellets, weighing 4.16 and 14.93 mg respectively in order to check the reproducibility of the measurements. The relative uncertainties of the Cp values were estimated at ±2 % for T > 50 K and ±5 % for lower temperatures, according to the results from Dachs and Benisek (2011) obtained for several standard reference powder samples encapsulated in Al-pans.

Moreover, the heat capacities of the dehydrated Ca-saturated ISCz-1 sample were also measured by using differential scanning calorimetry (DSC), between 300 and 520 K. The apparatus was a Calvet DSC111 from Setaram. The amount of dehydrated sample was 140.03 mg. The experimental procedure used for the C_p^0 measurements was described in Gailhanou et al. (2012).

2.3.2. Acid solution calorimetry at 298.15 K

The enthalpies of dissolution of the dehydrated ISCz-1 sample and of the fourteen illite/smectite samples from the Shinzan area were measured by isothermal dissolution calorimetry at 298.15 K in HF-HNO_3 solutions. The apparatus was a highly sensitive Tian-Calvet calorimeter, the Calsol calorimeter (Ganteaume et al., 1991). The calorimeter was calibrated by dissolving THAM (tris amino-2 hydroxymethyl-2 propanediol-1,3) crystal in a solution of hydrochloric acid (0.12 M), in the same conditions as for the experiments of Ganteaume et al. (1991). The experimental procedure for the measurements was described in details in Gailhanou et al. (2012). The acid solution compositions were HF(13M)-HNO_3(2M) for the ISCz-1 sample, and HF(3M)-HNO_3(2M) for the illite/smectite samples from the Shinzan area. A higher HF concentration was necessary in the case of the ISCz-1 sample compared with the other samples, because of the presence of a quite high amount of quartz (5.85 wt.%) in the ISCz-1 sample. The compositions of the acid solutions were optimized to obtain the complete dissolution of the samples after stirring at 540 rpm during about 3 hours. For the series of I/S samples from Shinzan area, about 20 mg to 30 mg of samples were dissolved in 50 mL of acid solution. For the dehydrated ISCz-1 sample, the amount of sample was about 40 mg for 50 mL of acid solution. The weighing of this latter sample and the filling of the sample vessel were carried out in a glove box under dry argon atmosphere in order to prevent from the hydration of the sample.

2.3.3. Standard enthalpy of formation of a clay mineral from constituents at 298.15 K

The experimental method described in Gailhanou et al. (2012, 2013) was used for the determination of the enthalpy of formation of the illite/smectite in the ISCz-1 sample. It was based on a set of dissolution reactions performed in order to obtain the enthalpy of formation of the clay mineral from secondary references, i.e. constituents chosen among oxides, hydroxides and nitrates, at 298.15 K. The reactions involved were (i) the dissolution of the clay sample, containing the clay mineral and impurities, (ii) the dissolution of a mixture composed of secondary references and of impurities with the same composition of those present in the sample and (iii) dilution type reactions. The masses of constituents (except H_2O), and impurities are calculated to present the elemental stoichiometry of 40 mg of anhydrous clay sample. The impurities were added to the mixture of constituents in the same amounts than those present in the clay sample. The weighings were realized in air atmosphere for a better stability of the balance, with a maximum deviation of 10 µg. Thus, about 46 mg of a mechanical mixture of constituents and impurities was made for each dissolution experiment to accurately determine the amounts of each of these compounds present in the mixture. Four or five measurements of enthalpies of dissolution were performed on each clay sample and constituents and impurities mixtures. Relative uncertainties for enthalpy values are lower than 0.5%. For a given sample, slight variations in the final solution composition existed due to the slight variations in sample mass. However, no dependency of the enthalpy of dissolution (per unit mass) on these variations of solution composition was observed.

The reaction of formation of a clay mineral from the constituents is expressed by (Gailhanou et al., 2013):

$$\sum_i n_i \ constituent_i^* + n_{H_2O} H_2O \rightarrow clay, n\ H_2O + n_{HNO_3}\ HNO_3 \qquad (1)$$

The superscript (*) refers to all constituents except H_2O, n_i is the amount of constituent *i* (in mol/mol of clay), n_{H2O} is the amount of constituent H_2O, obtained indirectly from the balance on O and H elements, *n* is the amount of water adsorbed in the clay, and n_{HNO3} is the amount of HNO_3, calculated from the balance on nitrates.

Therefore, the enthalpy of formation of the clay mineral from constituents $\Delta H^0_{f/constit}$ expressed in kJ/mol $O_{10}(OH)_2$ may be calculated according to the following formula described in Gailhanou et al. (2013):

$$\Delta H^0_{f/constit} = \left(\frac{M_{\min}}{\eta} + (n - n_{H2O})\, M_{H_2O} + n_{HNO_3} M_{HNO_3}\right)\Delta H_{diss,mixt} - \left(\frac{M_{\min}}{\eta} + n\, M_{H_2O}\right)\Delta H_{diss,sample} + n_{H2O}\, M_{H_2O}\, \Delta H_{dil} - n_{HNO3}\, M_{HNO_3}\Delta H_{sol} \quad (2)$$

where $M_{\min}$ is the molar mass of the dehydrated clay mineral, η is the mass fraction of dehydrated clay in the dehydrated sample, $\Delta H_{diss,mixt}$. is the enthalpy of dissolution of the constituents and impurities mixture (in J/g), and $\Delta H_{diss,sample}$ the enthalpy of dissolution of the clay sample (in J/g), ΔH_{dil} and ΔH_{sol} expressed in J/mol are respectively, the enthalpy of dilution of the HF-HNO_3 solution and the integral enthalpy of mixing of pure HNO_3 in HF-HNO3 solution.

Finally, the standard enthalpy of formation ΔH^0_f of the illite/smectite mineral was determined by considering $\Delta H^0_{f/constit}$ and the standard enthalpies of formation of the chosen secondary references.

3. RESULTS

3.1. Thermodynamic properties of anhydrous illite-smectite ISCz-1

3.1.1. Heat capacities

The heat capacities measured for the Ca saturated ISCz-1 sample are plotted between 2 and 330 K for PPMS data and between 300 and 520 K for DSC data (Figure 5). All the raw data are given in Electronic Annex EA-1. A significant discrepancy between the measurements performed by both techniques appears in the common temperature range 300 – 330K. By comparison with the Cp data obtained previously for the Na-saturated ISCz-1 sample (Gailhanou et al., 2007), the Cp values measured by DSC increase similarly, whereas the Cp values from PPMS tend to drastically discard from the general trend, between about 230 K and 330 K. This comparison with the Na-saturated ISCz-1 sample reveals an inaccuracy of the Cp values measured by PPMS at the highest temperature range. This could possibly be due to the low thermal conductivity of the sample. Indeed, Kennedy et al. (2007) tested the reliability of PPMS technique on several

phases and noticed that the Cp data could be precise but inaccurate at high temperature (T > 150 K) in the particular case of poor thermal conductor phases. Therefore, the heat capacities were interpolated between 200 and 520 °K using a least-square fit method and the polynomial function : $C_p(T) = 2.7070 - 3.1540 \cdot 10^{-4} T + 1.2571 \cdot 10^{4}\ T^{-2} - 33.827 T^{-0.5}$. Relative errors for the least square fit method are lower than 2 % at T > 300K.

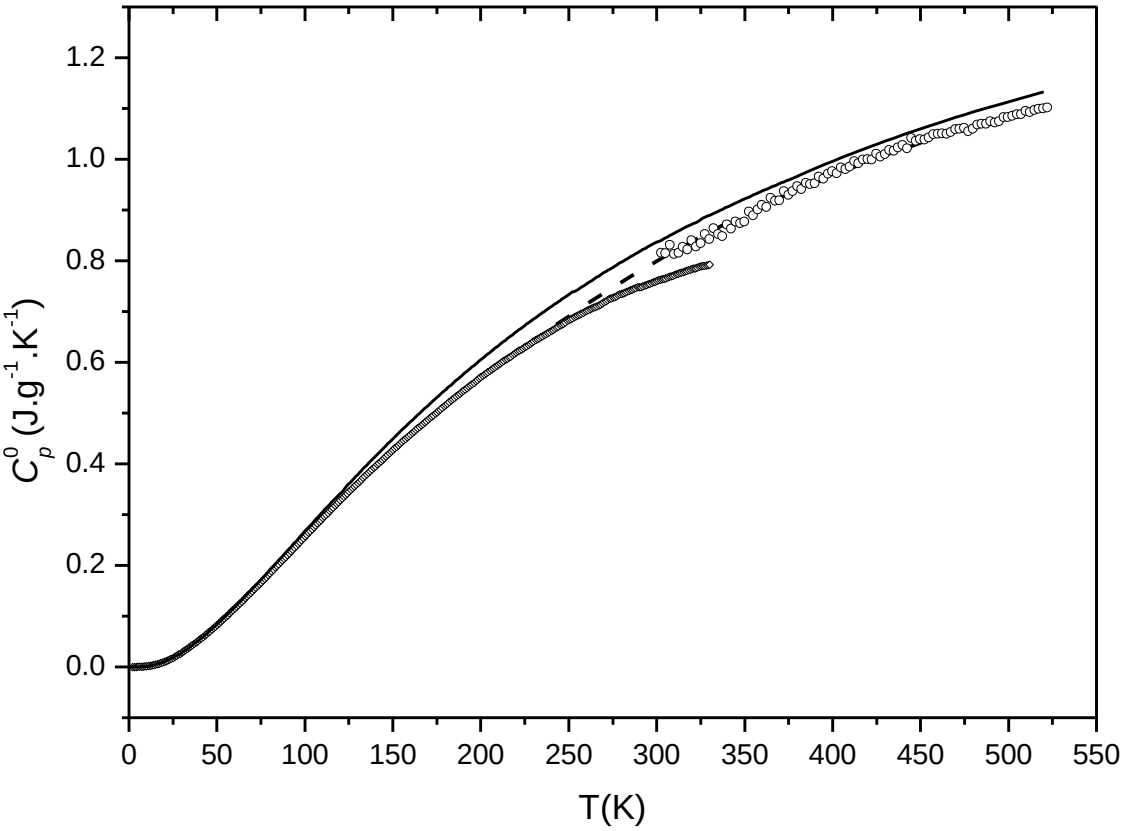

Figure 5. Heat capacities measured for ISCz-1(Ca) sample (diamonds : by PPMS; white circles: by DSC; dashed line: interpolated data) and ISCz-1(Na) sample (line : data from Gailhanou et al., 2007), between 2 K and 520 K.

The heat capacities of the clay sample are linearly interpolated at every degree between 0 and 520 °K. The heat capacities of the interstratified mineral are then calculated from the heat capacities of the sample by subtracting the contributions of the impurities (Table 4) according to the method described in Gailhanou et al. (2007). The heat capacity data for the impurities are taken from the literature (see references in EA-2). Because of the lack of thermodynamic data for the bernalite ($Fe(OH)_3$) mineral, this latter was assimilated to

goethite (FeOOH), for the correction calculations. Therefore, the amount of goethite considered in the following was adjusted to 0.98 wt.%, regarding the total amount of Fe in goethite and bernalite. Besides, the heat capacity data for goethite provided by Majzlan et al. (2003) are limited to the temperature range 0 – 375 °K, due to the occurrence of the magnetic Neel transition at about 375 °K. Consequently, the correction of the heat capacities of the sample is performed between 0 and 375 °K. The heat capacities of the interstratified mineral, $C_{p,m}^0$ expressed in J.mol^{-1}.K^{-1}, are given in Table 7 for this temperature range.

3.1.2. Heat contents

The heat contents of the mineral, $H^0(T) - H^0(298.15\,K)$, are calculated at any temperature by integration of the $C_{p,m}^0$ function, according to

$$H^0(T) - H^0(298.15\,K) = \int_{298.15}^{T} C_{p,m}^0 dT \quad (3)$$

using the trapezoid method at every degree (Table 7).

3.1.3. Entropy

The third-law entropy of the interstratified mineral, S^0, is expressed by

$$S^0 = \int_0^T \frac{C_{p,m}^0}{T} dT + S^{0(resid.)} \quad (4)$$

with $S^{0(cal)} = \int_0^T \frac{C_{p,m}^0}{T} dT$ the calorimetric entropy obtained directly from the heat capacity measurements, and $S^{0(resid)}$, the residual entropy. This latter term is not available from the calorimetric measurements and requires additional structural information about the mineral (Ulbrich and Waldbaum, 1976). The chemical site configurational entropy, $S^{0(conf)}$, associated with cationic disorder in the tetrahedral, octahedral and interlayer crystallographic sites, is a significant part of the residual entropy. It is assessed according to the method described in Blanc et al. (2015). The residual entropy may also include a magnetic term $S^{0(mag)}$ associated with the disordering of magnetic spins of transition metals in the clay minerals, occurring at very low temperatures (e.g. T < 10 K for iron-bearing chlorites, Townsend at al., 1986). Indeed, for clay minerals, recent studies (Gailhanou et al., 2009) have demonstrated that the magnetic contribution is difficult to detect

and to measure directly. A maximum value of the magnetic entropy is assessed by using the method described by Ulbrich and Waldbaum (1976), based on the maximum number of spin configurations according to:

$$S^{0(mag)} = R\sum_i x_i \ln(2S_i + 1) \quad (5)$$

where R is the gas constant, x_i the amount of element *i* and S_i its spin number (for Fe^{3+}, $S = 5/2$; for Fe^{2+}, $S = 2$). Finally, in the case of the illite-smectite ISCz-1 mineral, the configurational entropy $S^{0(conf)}$ is estimated at 23.19 $J.mol^{-1}.K^{-1}$ and the maximum magnetic entropy, at 0.65 $J.mol^{-1}.K^{-1}$. The calorimetric entropy data are given in Table 7.

Table 7. Molar heat capacities and derived thermodynamic functions of the dehydrated Ca-saturated illite-smectite ISCz-1 mineral (corrected for impurities) at selected temperatures.

T	$C^0_{p,m}(T)$	$S^{(0)cal}$	$H^0(T) - H^0(298.15)$
K	$J.mol^{-1}.K^{-1}$	$J.mol^{-1}.K^{-1}$	$kJ.mol^{-1}$
0	0.00	0.00	-45.596
10	0.65	0.42	-45.594
20	3.81	1.65	-45.574
30	10.61	4.37	-45.505
40	19.85	8.64	-45.354
50	30.53	14.20	-45.103
60	43.01	20.85	-44.736
70	55.96	28.44	-44.242
80	69.39	36.78	-43.616
90	83.08	45.75	-42.853
100	97.33	55.24	-41.951
110	111.25	65.17	-40.908
120	124.93	75.43	-39.728
130	138.00	85.95	-38.413
140	150.81	96.66	-36.968
150	163.30	107.49	-35.397
160	175.05	118.41	-33.704
170	186.45	129.37	-31.896
180	197.55	140.34	-29.976
190	208.35	151.31	-27.946
200	216.66	162.25	-25.812
210	226.42	173.06	-23.597
220	236.19	183.82	-21.284
230	245.88	194.53	-18.873
240	255.41	205.20	-16.367
250	264.72	215.81	-13.766
260	273.81	226.38	-11.073
270	282.64	236.88	-8.291
280	291.20	247.31	-5.421
290	299.49	257.67	-2.468
298.15	306.05	266.06	0.000
300	307.51	267.96	0.568
310	315.23	278.17	3.682

320	322.66	288.30	6.871
330	329.83	298.34	10.134
340	336.73	308.29	13.467
350	343.37	318.14	16.868
360	349.78	327.91	20.334
370	355.95	337.58	23.862
375	358.95	342.37	25.650

3.1.4. Standard enthalpy of formation

Enthalpies of dissolution of the Ca-saturated ISCz-1 sample and of the constituents* mixture (superscript * means: except H_2O constituent) are given in Table 8. Uncertainties associated with the mean enthalpies are calculated from measured values using Student's *t*-distribution with a 95 percent-confidence interval.

Table 8. Enthalpies of dissolution of the dehydrated ISCz-1 sample and of the corresponding constituents and impurities mixtures

		Mass (mg)	ΔH_{diss} (J/g)	Mean ΔH_{diss} (J/g)
ISCz-1 in HF(13M)-HNO_3(2M)	Dehydrated sample ISCz-1	39.86	-2256.60	-2257.82 (±1.19)
		40.01	-2257.62	
		40.00	-2258.31	
		40.20	-2258.74	
	Mixture of constituents* + impurities	46.58	-1845.16	-1848.08 (±3.28)
		46.55	-1849.41	
		46.55	-1850.65	
		46.57	-1845.16	
		46.55	-1850.00	

Note: Uncertainties between brackets are calculated using Student's *t*-distribution with a 95% confidence interval

The enthalpy of dilution ΔH_{dil} and the solution enthalpy ΔH_{sol} associated with the mixing of pure HNO_3 in HF(13M) - HNO_3(2M) were determined in Gailhanou et al. (2012). Their values were respectively -1.57 (± 0.30) kJ.mol^{-1} H_2O and -27.7 (± 26) kJ.mol^{-1} HNO_3.

Afterwards, the enthalpy of formation of the mineral from constituents was then calculated using equation (2) (Table 9).

Table 9. Reaction of formation of illite-smectite ISCz-1 from the secondary reference constituents and associated enthalpy $\Delta H°_{f/constit.}$, in kJ.mol^{-1} (at 1 bar and 298.15 K).

Reactions of formation of mixed-layer mineral	$\Delta H°_{f/constit.}$ (kJ.mol^{-1})

Illite/smectite ISCz-1 (n = 0)	3.562 $SiO_{2,quartz}$ + 2.159 $Al(OH)_{3,gibbsite}$ + 0.255 $Mg(OH)_2$ + 0.029 $FeOOH_{,goethite}$ + 0.011 FeO + 0.008 $TiO_{2,rutile}$ + 0.440 KNO_3 + 0.092 $Ca(OH)_2$ = $(Ca_{0.092}K_{0.440})(Si_{3.562}Al_{0.438})(Al_{1.721}Mg_{0.255}Fe^{3+}_{0.029}Fe^{2+}_{0.011}Ti_{0.008})O_{10}(OH)_2$ +0.440 HNO_3 +2.380 H_2O	62.36 (±3.49)

Notes: M_{min}(ISCz-1) = 382.007 g.mol^{-1}; η(ISCz-1) = 0.88456; M_{H2O} = 18.02 g.mol^{-1}; M_{HNO3} = 63.01 g.mol^{-1} ; n_{H2O} = -2.380 ; n = 0 ; n_{HNO3} = 0.440.
Standard uncertainties given between brackets correspond to one standard deviation of the means.

Eventually, the standard enthalpy of formation of the illite-smectite ΔH_f^0 was obtained from the enthalpy of formation of the mineral from the secondary reference constituents and from the standard enthalpies of formation of these reference constituents (Table 10). These latter values are selected consistently with the Thermochimie database (Giffaut et al., 2014), at 298.15 K, and are tabulated in Electronic Annex EA-3.

The uncertainty associated with ΔH_f^0 was standard deviation of the mean, calculated using the error propagation method (Ellison et al., 2000):

$$\Delta(\Delta H_f^0) = \sqrt{\left[\Delta(\Delta H_{f/constit.}^0)\right]^2 + \sum_i \nu_i^2 \left[\Delta(\Delta H_f^{constit.i})\right]^2} \quad (3)$$

Where ν_i is the stoichiometric coefficient associated with the constituent *i*, and $\Delta H_f^{constit.i}$ is the standard enthalpy of formation of the constituent *i*. The uncertainties associated with $\Delta H_{f/constit.}^0$ and $\Delta H_f^{constit.i}$ correspond to one standard deviation of the mean.

3.1.5. Standard Gibbs free energy of formation

The standard Gibbs free energy of formation ΔG_f^0 is expressed by:

$$\Delta G_f^0(T) = \Delta H_f^0(T) - T\Delta S_f^0(T) \quad (4)$$

where $\Delta S_f^0(T)$ is the standard entropy of formation of the interstratified mineral calculated considering the reaction of formation of the mineral from the elements in their stable thermodynamic form in standard conditions. The value for the ISCz-1 mineral was obtained at 298.15 K from the third-law entropy of the mineral S^0 (Table 10) and from the entropies of the elements at 298.15 K. These latter data were taken from Cox et al. (1989) for $Si_{(cr)}$, $Al_{(cr)}$, $Mg_{(cr)}$,$Ti_{(cr)}$, $K_{(cr)}$, $Ca_{(cr)}$, $O_{2(g)}$, $H_{2(g)}$ and from Chase (1998) for $Fe_{(cr)}$.

3.2. Synthesis of the thermodynamic properties for anhydrous illite-smectite ISCz-1

The complete set of thermodynamic properties of the interstratified ISCz-1 mineral at 1 bar and 298.15 K is given in Table 10. Since its structural formula contains a small amount of TiO_2, a simplified structural formula is also proposed in order to ease the introduction of the phase into geochemical databases. The simplification is based on fictive solid-solid reactions with properties of reaction equal to 0. In the case of the interstratified ISCz-1, the following fictive reaction was considered :

$$(Ca_{0.092}K_{0.440})(Si_{3.562}Al_{0.438})(Al_{1.721}Mg_{0.255}Fe^{3+}_{0.029}Fe^{2+}_{0.011}Ti_{0.008})O_{10}(OH)_2 + 0.0055\ Al_2O_3 = (Ca_{0.092}K_{0.439})(Si_{3.562}Al_{0.438})(Al_{1.732}Mg_{0.255}Fe^{3+}_{0.029}Fe^{2+}_{0.011})O_{10}(OH)_2 + 0.0005\ K_2O + 0.008\ TiO_2 \quad (5)$$

The thermodynamic data for alumina-α, rutile and K_2O are taken from the Thermoddem database (http://thermoddem.brgm.fr, Blanc et al. (2012)).

Table 10. Thermodynamic properties of the dehydrated illite-smectite ISCz-1 mineral, at 1 bar and 298.15 K.

	T = 298.15 K								A	B*10^3	C*10^{-5}	T range for C_p functions
Mineral	ΔG_f^0 (kJ mol^{-1})	ΔH_f^0 (kJ mol^{-1})	$S^{(cal)0}$ (J mol^{-1} K^{-1})	$S^{(conf)0}$ (J mol^{-1} K^{-1})	$S^{(mag)0}$ (J mol^{-1} K^{-1})	S^0 (J mol^{-1} K^{-1})	$V^{0\perp}$ (cm^3 mol^{-1})	C_p (298.15 K) (J mol^{-1} K^{-1})	J/(mol K)	J/(mol K^2)	(J K /mol)	
Illite/smectite ISCz-1	-5417.38 (± 7.60)	-5785.74 (± 7.46)	266.06	29.53	0.58	296.17	137.13	306.05	228.34	438.31	-47.04	298 – 375 K
Properties recalculated for a simplified structural formula‡												
Illite/smectite ISCz-1*	-5418.62 (± 7.60)	-5787.22 (± 7.46)	265.89	28.89	0.58	295.36	137.13	306.00	236.14	422.80	-49.92	298 – 375 K

Notes: Between 298 and 375 K, Cp(T) functions are expressed according to Cp(T) = A + B 10^{-3} T + C 10^5 T^{-2}, where A, B and C are Maier-Kelley coefficients, obtained by fitting the Cp curves.

Standard uncertainties associated with ΔH_f^0 and ΔG_f^0 correspond to one standard deviation of the means (see text for details).

$^{\perp}$ Molar volume V^0 is obtained from values of unit-cell parameters a, b and c determined from XRD patterns, according to the method described in Gailhanou et al. (2012): for the present dehydrated ISCz-1 sample, a = 5.20 Å , b = 9.01 Å and c = 10.12 Å.

‡ Simplified formula is introduced to ease the predictive calculations and their implementation into databases. The simplification process is detailed in the text.

Illite/smectite ISCz-1: $(Ca_{0.092}K_{0.440})(Si_{3.562}Al_{0.438})(Al_{1.721}Mg_{0.255}Fe^{3+}_{0.029}Fe^{2+}_{0.011}Ti_{0.008})O_{10}(OH)_2$

Illite/smectite ISCz-1*: $(Ca_{0.092}K_{0.439})(Si_{3.562}Al_{0.438})(Al_{1.732}Mg_{0.255}Fe^{3+}_{0.029}Fe^{2+}_{0.011})O_{10}(OH)_2$

3.3. Enthalpies of mixing for mixed-layers from Shinzan area samples

The analysis of the chemical dispersions among the illite-smectite compositions (Figure 4) shows that all of these one can be described by a ternary solid solution, with illite N, montmorillonite A and illite-smectite F end members. Although the chemical dispersions occur mostly along the illite – smectite join, the ternary solid solution is preferred to the binary illite-smectite solid solution for accuracy reasons. Since the enthalpies of mixing are expected to be very low, and consequently difficult to determine accurately regarding the associated uncertainties, it is preferable to perform the measurements for all the samples without adding a supplementary source of uncertainty induced by the consideration of the binary solid solution. In the following, the enthalpies of mixing for illite-smectite compositions from the Shinzan area samples are determined by using isothermal dissolution calorimetry at 298.15 K.

3.3.1. Enthalpies of dissolution at 298.15 K

The enthalpies of dissolution of all the samples in HF(3M)-HNO_3(2M) at 25 °C were measured by Perbost et al. (2002). The data are given in

Table 11. Uncertainties associated with the mean enthalpies are calculated from measured values using Student's *t*-distribution with a 95 percent-confidence interval. The relative uncertainties are lower than 1%, except for the sample E, at 2.4%.

Table 11. Mean values of the enthalpies of dissolution of the I/S samples from Shinzan area, measured by Perbost et al. (2002) in HF(3M)-HNO3(2M) solution at 25 °C. Mnt A = Montmorillonite A. Uncertainties calculated using Student's *t*-distribution with a 95 percent-confidence interval.

Sample	Mean value of ΔH_{diss} ($kJ.mol^{-1}$)
Mnt A	-846.80 (± 7.64)
B	-844.03 (± 1.45)
C	-859.94
D	-847.84 (± 2.95)
E	-842.04 (± 20.2)
F	-840.77 (± 2.52)
G	-859.50
H	-848.02 (± 6.14)
I	-860.21
J	-866.77
K	-854.33
L	-858.14
M	-863.52
Illite N	-863.57 (± 6.39)

The opposite values of the enthalpies of dissolution are plotted in

Figure **6**a, in the 3-D space ($\mathbf{F_1}$, $\mathbf{F_2}$, $-\Delta H_{diss}$). The values were then modelled by a polynomial surface, by using the least-square fit method. The polynomial function is expressed by:

$$P(z_1,z_2) = 852.124 - 6.029\ z_1 + 41.159\ z_2 + 1.938\ z_1^2 - 4.027\ z_1z_2 + 45.824\ z_2^2 \quad (6)$$

where z_1 and z_2 correspond to the coordinates of the I/S samples in the ($\mathbf{F_1}$,$\mathbf{F_2}$) plane.

The discrepancies between the measured and modelled values are lower than 1%, which corresponds to the relative uncertainties for the measured enthalpies of dissolution. The modelled values are then considered to represent correctly the measured enthalpies.

3.3.2. Enthalpies of mixing at 298.15 K

The illite-smectite compositions may be expressed by a linear combination of the compositions of the three end-members A, F and N. The barycentric coordinates (a_A, a_F, a_N) for all the I/S samples are given in Table 12. With respect to these end-members, the enthalpy of mixing for an interstratified X from the Shinzan series is the enthalpy of the reaction of formation:

$$a_A\ Mnt\ A + a_N\ illite\ N + a_F\ mixed layer\ F \rightarrow mixed layer\ X \quad (7)$$

which practically represents the enthalpy of mixing of illite and smectite (montmorillonite) layers. The enthalpy of mixing is then obtained from the combination of the reactions of dissolution of the minerals and is expressed by:

$$\Delta H_m(mixed layer\ X) = a_A \Delta H_{diss}(A) + a_N \Delta H_{diss}(N) + a_F \Delta H_{diss}(F) - \Delta H_{diss}(mixed layer\ X) + \Delta H_{mix,sol} \quad (8)$$

where $\Delta H_{mix,sol}$ is the enthalpy of mixing of solutions resulting from the dissolution reactions of the minerals, which is neglected in the following calculations. The enthalpies of mixing are then calculated for all the illite-smectite compositions, from the modelled values of the enthalpies of dissolution (

Table **12**), and are plotted in the (**F_1**, **F_2**, ΔH_m,) space (

Figure **6**b).

Table 12. Enthalpies of mixing of the I/S minerals from the Shinzan area, with respect to the three end-members Mnt A, illite N and interstratified F. a_A, a_N and a_F are the barycentric coordinates of the I/S minerals, associated with the corresponding end-members.

Samples	a_A	a_N	a_F	ΔH_m (kJ.mol^{-1})
Mnt A	1.00	0.00	0.00	0.00
B	0.85	-0.06	0.20	0.20
C	0.68	0.02	0.30	-0.99

D	0.66	0.21	0.13	-2.64
E	0.53	0.29	0.18	-3.18
F	0.00	0.00	1.00	0.00
G	0.97	0.58	-0.55	-2.98
H	0.50	0.52	-0.02	-3.70
I	0.40	0.47	0.12	-3.62
J	0.74	0.85	-0.59	-2.41
K	-0.25	0.48	0.77	-1.47
L	-0.02	0.69	0.33	-2.19
M	0.01	0.85	0.14	-1.39
Illite N	0.00	1.00	0.00	0.00

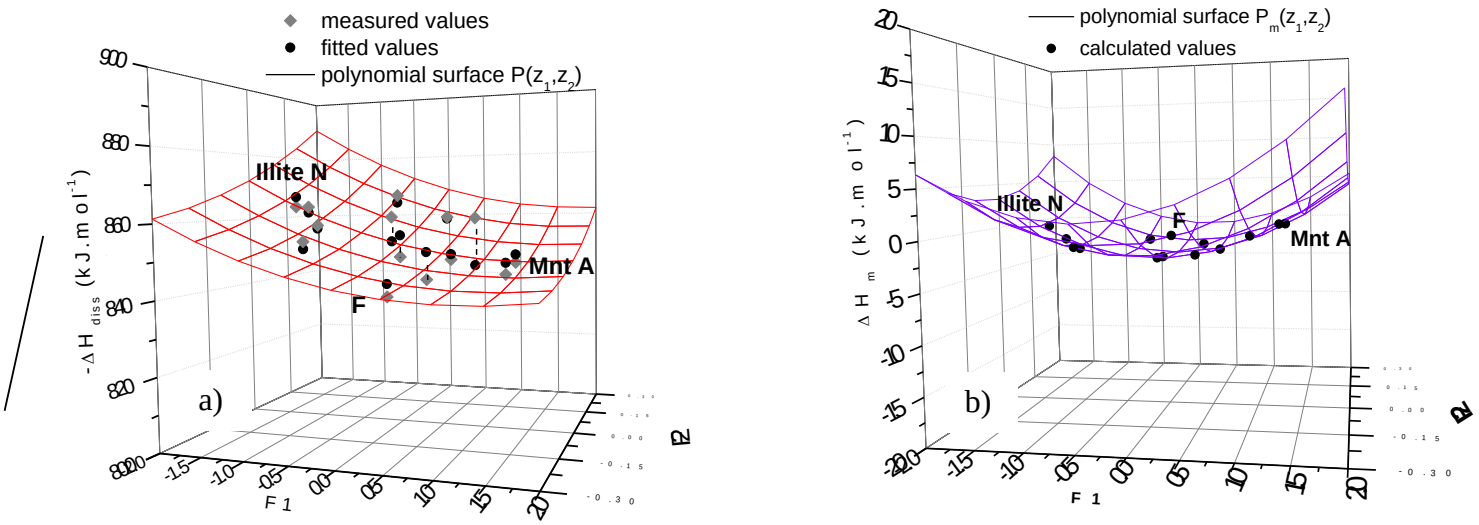

Figure 6. Representations of (a) the polynomial surface $P(z_1,z_2)$ obtained by fitting the experimental values of $-\Delta H_{diss}$ for the I/S samples and (b) the enthalpies of mixing of the illite and smectite layers (per mol $O_{10}(OH)_2$) for the I/S minerals and the modelling polynomial surface $P_m(z_1,z_2)$.

The resulting enthalpies of mixing are slightly negative, with a minimum value at about -3.7 kJ.mol^{-1} for the H and I samples. According to XRD modelling (Inoue and Utada, 1983), these latter are first order R1 type and should contain about 30-35 % of smectite layers. A model predicting ΔH_m was proposed by Blanc et al. (1997), resulting in ΔH_m = -3.6 kJ.mol^{-1} for illite/smectite displaying such composition and ordering types.

563

4. DISCUSSION: comparison with estimates and stability domains

The standard thermodynamic properties of the illite-smectite ISCz-1 obtained experimentally are compared with estimated values calculated from Blanc et al. (2015) model that includes a consistent set of models for predicting the standard thermodynamic properties (H, S, Cp, V) for phyllosilicates. First, the model from Blanc et al. (2015) is merely applied by considering the whole structural formula of the illite-smectite. The simplified structural formula, $(Ca_{0.092}K_{0.439})(Si_{3.562}Al_{0.438})(Al_{1.732}Mg_{0.255}Fe^{3+}_{0.029}Fe^{2+}_{0.011})O_{10}(OH)_{2,}$ is considered in order to ease the predictive calculations. Results are given in Table 13. Besides, a second approach is carried out, predicting separately the thermodynamic parameters of illite and smectite components and combining them according to the required composition of illite-smectite. This approach aims to differentiate the chemistry of the illite and smectite layers in the interstratified, consistently with the structure of the mineral illite-smectite.

The method for calculating the chemical compositions of illite and smectite end-members relies on the work of Meunier and Velde (1989), based on the graphical representation of M^{+}-4Si-R^{2+} ternary system for natural sample compositions. Plotting ISCz-1 coordinates in such a diagram (Figure 7) reveals that illite-smectite ISCz-1 can be considered as a binary solid solution with a high-charge illite ($0.87/O_{10}(OH)_2$), namely IllitePP, and a low-charge montmorillonite (0.21), namely MontmorillonitePP, end-members. Meunier and Velde (1989) have proposed relations between illite and montmorillonite theoretical end-members. The compositions of the end-members are deduced from their coordinates in the M^{+}-4Si-R^{2+} triangle, which provide chemical constraints, and from a calculation based on a least-square method to adjust the proportions of illite and smectite components. These latter were determined considering 70% of illite, consistently with the proportions obtained from XRD. Finally, the thermodynamic properties of the illite and smectite end-members are calculated by using the model from Blanc et al. (2015) for each end-members, then considering a linear combination of both. The set of data is completed by considering the mixing enthalpy measured for the I/S sample with 70% of illite layers (sample I, Table 5), -3.6 $kJ.mol^{-1}$.

Regarding the results (reported in Table 13) , the prediction obtained by considering the mixture of illite and smectite components falls closest to the experimental values except for heat capacity and volume. For these latter properties, both estimate method provide similar results and, on the whole, the method based on a mixture of layers is slightly improving the accuracy of the predictions for the properties of illite-smectite ISCz-1 mineral.

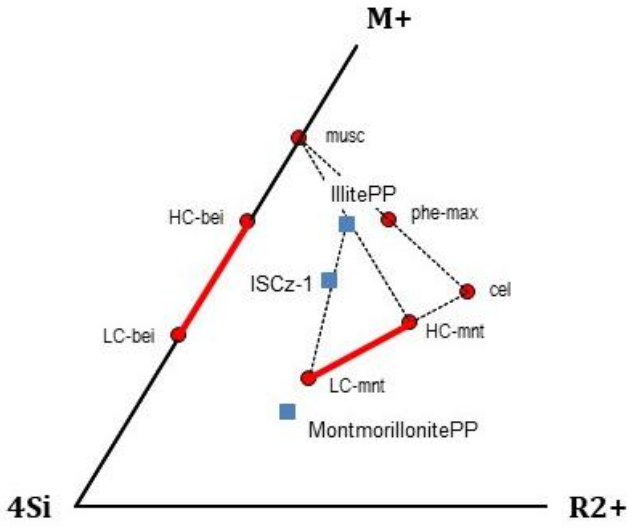

Figure 7. Composition of clay minerals in the M^{+}-4Si-R^{2+} system (M^{+} = layer charge of ideal mica, 4Si = Si content of the tetrahedral sheet, R^{2+} = amount of bivalent cations in the octahedral position). Musc = Muscovite, phe-max = Phengite, cel = celadonite, IllitePP = illite end-member (layer charge 0.87), HC-mnt = high charge montmorillonite, LC-mnt = low charge montmorillonite, beid = beidellite. IllitePP and MontmorillonitePP are the predicted compositions of the illite and smectite components in the mixed-layer ISCz-1.

Table 13. Estimated thermodynamic properties of ISCz-1, at 1 bar and 298.15K, according to the model from Blanc et al. (2015). Data are compared with the experimental values obtained for the simplified structural formula, given in Table 11.

Predicted	ΔG_f^0 kJ.mol^{-1}	ΔH_f^0 kJ.mol^{-1}	$S^{0(tot)}$ J.mol^{-1}.K^{-1}	$C_p{}^0$(298.15 K) J.mol^{-1}.K^{-1}	V cm^3.mol^{-1}
Mean composition	-5412.63	-5779.31	301.78	317.63	137.94
Δ(exp-pred)	-5.99	-7.91	-6.41	-11.58	-0.81
Δ (%)	-0.11	-0.13	-2.17	-3.78	-0.59
Mix illite/smectite layers*	-5415.19	-5785.52	290.03	317.79	138.00
Mixing terms	-3.6	-3.6			
Final estimate	-5418.89	-5789.22	290.03	317.79	138.00
Δ(exp-pred)	0.17	1.90	5.33	-11.74	-0.87
Δ (%)	0.00	0.03	1.80	-3.80	-0.63

*illite component : $K_{0.683}Ca_{0.084}(Si_{3.319}Al_{0.681})(Al_{1.777}Mg_{0.234}Fe^{2+}_{0.016})O_{10}(OH)_2$
smectite component : $Ca_{0.107}Si_4(Al_{1.652}Mg_{0.292}Fe^{3+}_{0.081}Fe^{2+}_{0.003})O_{10}(OH)_2$

As stated by Blanc et al. (1997), the mixing of layers introduces an additional entropy term, which is not measurable directly by calorimetry, for instance. Blanc et al. (1997) have proposed a predicting model based on nearest neighbor interaction up to the fourth neighbor. In a simpler approach, we can first state for an ideal solid solution between illite and smectite end members, which would result, for ISCz-1 with 70 % illite, in $\Delta S_m = 5.38$ J.mol^{-1}.K^{-1}.

In Figure 8, the stability fields for ISCz-1, Illite and Montmorillonite end-members are drawn at 25°C, considering two different sets of thermodynamic parameters for ISCz-1:

- a set including ΔH_m for ISCz-1 properties of formation (Figure 8.A)
- a set excluding ΔH_m for ISCz-1 properties of formation (Figure 8.B).

Comparing Fig. 8.A and Fig. 8.B enlighten the importance of mixing terms. Indeed, ISCz-1 stability field just disappears when the mixing terms are not integrated to the thermodynamics function, whereas it lies as expected between illite and montmorillonite end members when the mixing terms are added to the ISCz-1 formation properties. On the whole, in the calculation process followed here to predict the thermodynamic properties of illite/smectite, we consider a mixture of layers, with the composition of the montmorillonite component being itself raging between high and low charge montmorillonite, consistently with Meunier and Velde (1989). As can be seen from Fig. 8 a simple mixture is not sufficient and additional and mixing terms are necessary to result in a significant stability, ranging as expected between illite and montmorillonite end members.

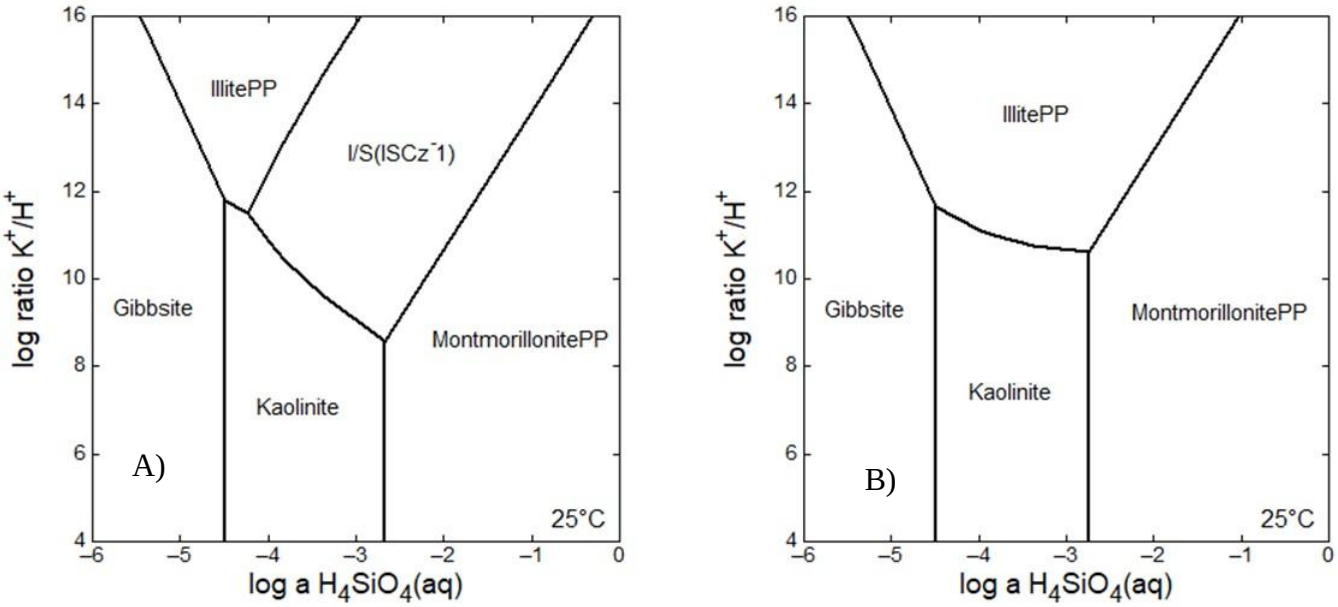

Figure 8 – Stability fields for I/S ISCz-1 mineral: A) including enthalpy of mixing and B) without enthalpy of mixing.

5. SUMMARY AND CONCLUSIONS

In early diagenesis and underground storage studies, the transformation of smectite into illite has been recognized for long to involve the formation of interstratified illite/smectite as intermediate product (Srodon and Eberl, 1984, Meunier and Velde, 1989). However the lack of thermodynamic properties prevented it to be implemented into geochemical calculations, so far. This study presents the first calorimetric direct measurements of such properties.

The measurements were carried out onto a purified, Ca-saturated ISCz-1 sample from Slovakia, provided by the Source Clays Repository of the Clay Minerals Society. $\Delta H°f$ was obtained from acid solution calorimetry experiments, S° and Cp were measured by PPMS and DSC techniques. In addition, a specific mixing enthalpy was measured by acid solution calorimetry, considering samples from the Shinzan hydrothermal series (Inoue and Utada, 1983). For the whole set of measured thermodynamic properties, the comparison with previously published estimation method (Blanc et al., 2015) was favorable, provided the estimate is calculated distinguishing the respective contribution of illite and smectite layers. The respective compositions of these latter are derived from composition relations established by Meunier and Velde (1989).

Among the concluding points, comparing the different estimating methods brings out that the energetic terms for layer mixing are necessary for the mineral stability, even though their magnitude is small with respect to formation terms, i.e. even falling within the uncertainty obtained for the formation terms. This implies that further improvements and advances could be made by considering weak energies terms like hydration or exchange reaction contributions (Gailhanou et al., 2017).

Acknowledgements: Financial support from the French Radioactive Waste Management Agency (ANDRA), from the French Geological Survey (BRGM) and from the French National Council for Scientific Research (CNRS) is gratefully acknowledged. The authors thank Professor A. Inoue, Chiba University, for supplying the illite-smectite samples from the Shinzan Area.

6. REFERENCES

Amouric, M., Olives, J. (1991). Illitization of smectite as seen by high-resolution transmission electron microscopy. *Eur. J. Miner*. **3**, 831-835.

Blanc, P., Bieber, A., Fritz, B. and Duplay, J. (1997) A short range interaction model applied to illite/smectite mixed-layer minerals. *Phys. Chem. Miner.* **24**, 574-581.

Blanc, P., Legendre, O. and Gaucher, E.C. (2007) Estimate of clay minerals amounts from XRD pattern modeling: The Arquant model. *Phys. Chem. Earth* **23**, 135 - 144.

Blanc, P., Lassin, A., Piantone, P., Azaroual, M., Jacquemet, N., Fabbri, A. and Gaucher, E. C. (2012) Thermoddem: A geochemical database focused on low temperature water/rock interactions and waste materials. *App. Geochem.* **27**, 2107-2116.

Blanc, P., P. Vieillard, Gailhanou, H., Gaboreau, S., Gaucher, E., Fialips, C.I., Made, B. and Giffaut, E. (2015) A generalized model for predicting the thermodynamic properties of clay minerals. *Amer. J. Sci.* **315**, 734-780.

Chase, M.W.J. (1998). NIST-NAJAF thermochemical tables, 4th ed. National Institute of Standards and Technology, Washington D.C.

Chipera, S.J. and Bish, D.L. (2001) Baseline studies of the Clay Minerals Society Source Clays: powder X-ray diffraction analyses. *Clays Clay Miner*. **49**, 398-409.

Colton-Bratley,V.A.C. (1987). Role of pressure in smectite dehydration - effect on geopressure and smectite-to-illite transition. *A.A.P.G. Bull.* **53**, 73-93.

Cox, J.D., Wagman, D.D., Medvedev, V.A. (1989). CODATA Key Values for Thermodynamics. Hemisphere Publishing Corp., New York.

694 Cuadros, J. and Linares, J. (1996) Experimental kinetic study of the smectite-to-illite transformation.
695 *Geochim. Cosmochim. Acta* **60**, 439-453.

696 Dachs, E. and Benisek, A. (2011) A sample-saving method for heat capacity measurements on
697 powders using relaxation calorimetry. *Cryogenics* **51**, 460-464.

698 Dachs, E. and Bertoldi, C. (2005) Precision and accuracy of the heat-pulse calorimetric technique:
699 low-temperature heat capacities of milligram-sized synthetic mineral samples. *Eur. J. Miner.* **17**,
700 251-261.

701 Dauzeres, A., Le Bescop, P., Sardini, P., Cau Dit Coumes, C. (2010) Physico-chemical investigation
702 of clayey/cement-based materials interaction in the context of geological waste disposal:
703 Experimental approach and results. *Cem. Concr. Res.* **40**, 1327-1340.

704 Ellison S.L.R., Roesslein M. and Williams A. (Eds). (2000) EURACHEM/CITAC Guide: quantifying
705 uncertainty in analytical measurement, 2nd ed. EURACHEM. ISBN 0-948926-15-5.

706 Gailhanou, H., van Miltenburg, J.C., Rogez, J., Olives, J., Amouric, M., Gaucher, E.C. and Blanc, P.
707 (2007) Thermodynamic properties of anhydrous smectite MX-80, illite IMt-2 and mixed-layer illite-
708 smectite ISCz-1 as determined by calorimetric methods. Part I: Heat capacities, heat contents and
709 entropies. *Geochim. Cosmochim. Acta* **71**, 5463-5473.

710 Gailhanou, H., Rogez, J., Miltenburg, J.C.v., Genderen, A.C.G.v., Grenèche, J.M., Gilles, C.,
711 Jalabert, D., Michau, N., Gaucher, E.C. and Blanc, P. (2009). Thermodynamic properties of chlorite
712 CCa-2. Heat capacities, heat contents and entropies. *Geochim. Cosmochim. Acta* **73**, 4738-4749.

713 Gailhanou, H., Blanc, P., Rogez, J., Mikaelian, G., Kawaji, H., Olives, J., Amouric, M., Denoyel, R.,
714 Bourrelly, S., Montouillout, V., Vieillard, P., Fialips, C.I., Michau, N., Gaucher, E.C. (2012)
715 Thermodynamic properties of illite, smectite and beidellite by calorimetric methods: Enthalpies of
716 formation, heat capacities, entropies and Gibbs free energies of formation. *Geochim. Cosmochim.*
717 *Acta* **89**, 279-301.

718 Gailhanou, H., P. Blanc, Rogez, J., Mikaelian, G., Horiushi, K.,Yamamura, Y., Saito, K., Kawaji, H.,
719 Warmont, F., Grenèche, J. M., Vieillard, P., Fialips, C. I., Giffaut, E. and Gaucher, E.C. (2013).
720 Thermodynamic properties of saponite, nontronite, and vermiculite derived from calorimetric
721 measurements. *Amer. Miner.* **98**, 1834-1847.

722 Gailhanou, H., Vieillard, P., Blanc, P., Lassin, A., Denoyel, R., Bloch, E., De Weireld, G., Gaboreau,
723 S., Fialips, C.I., Madé, B. and Giffaut, E. (2017) Methodology for determining the thermodynamic
724 properties of smectite hydration. *App. Geochem.* **82**, 146-163.

725 Ganteaume, M., Coten, M. and Decressac, M. (1991) Un nouveau calorimètre en solution: le Calsol.
726 *Thermochim. Acta* **178**, 81-98.

727 Garg, N., Skibsted, J. (2016) Pozzolanic reactivity of a calcined interstratified illite/smectite (70/30)
728 clay. *Cem. Concr. Res.* **79**, 101–111.

729 Gaucher, E.C., Blanc, P., Matray, J.-M., Michau, N. (2004). Modeling diffusion of an alkaline plume
730 in a clay barrier. *App. Geochem.* **19**, 1505-1515.

731 Gaucher, E.C. and Blanc, P. (2006). Cement/clay interactions – A review: Experiments, natural
732 analogues, and modeling. *Waste Manage*. **26**, 776-788.

733 Gaucher, E.C., Tournassat, C., Pearson, F.J., Blanc, P., Crouzet, C., Lerouge, C. and Altmann, S.
734 (2009) A robust model for pore-water chemistry of clayrock. *Geochim. Cosmochim. Acta* **73**, 6470-
735 6487.

736 Giffaut, E., Grivé, M., Blanc, P., Vieillard, P., Colàs, E., Gailhanou, H., Gaboreau, S., Marty, N.,
737 Madé, B., Duro, L. (2014). Andra thermodynamic database for performance assessment:
738 ThermoChimie. *App. Geochem.* **49**, 225-236.

739 Guyonnet, D., Touze-Foltz, N., Norotte, V., Pothier, C., Didier, G., Gailhanou, H., Blanc, P. and
740 Warmont, F. (2009) Performance-based indicators for controlling geosynthetic clay liners in landfill
741 applications. *Geotext. Geomemb.* **27**, 321-331.

742 Hower, J., Eslinger, E.V., Hower, M , and Perry, E.A. (1976) Mechanism of burial metamorphism of
743 argillaceous sediments, l. Mineralogical and chemical evidence. *Geol. Soc. Amer. Bull*. **87**, 725-737

744 Inoue, A., and Utada, M (1983) Further investigations of a conversion series of dioctahedral
745 mica/smectites in the Shinzan hydrothermal alteration area, northeast Japan. *Clays Clay Miner.*
746 **31**,401-412.

747 Inoue, A., Kohyama, N., Kitagawa, R. and Watanabe, T. (1987) Chemical and morphological
748 evidence for the conversion of smectite to illite. *Clays Clay Miner*. **35**, 111-120.

749 Kennedy, C.A., Stancescu, M., Marriott, R.A. and White, M.A. (2007) Recommendations for
750 accurate heat capacity measurements using a Quantum Design physical property measurement
751 system. *Cryogenics* **47**, 107-112.

752 Lanson, B., Sakharov, B.A., Claret, F. and Drits, V.A. (2009). Diagenetic smectite-to-illite transition
753 in clay-rich sediments: A reappraisal of X-ray diffraction results using the multi-specimen method.
754 *Amer. J. Sci.* **309**, 476-516.

755 Majzlan J., Grevel K. D. and Navrotsky A. (2003) Thermodynamics of Fe oxides: Part II. Enthalpies
756 of formation and relative stability of goethite (α-FeOOH), lepidocrocite (γ-FeOOH), and maghemite
757 (γ-Fe_2O_3). *Amer. Miner.* **88**, 855–859.

758 Marty, N.M., Munier, I., Gaucher, E., Tournassat, C., Gaboreau, S., Vong, C., Giffaut, E., Cochepin,
759 B., Claret, F. (2014). Simulation of Cement/Clay Interactions: Feedback on the Increasing
760 Complexity of Modelling Strategies. *Transp. Porous Med.*, 1-21.

761 Massiot D., Fayon F., Capron M., King I., Le Calvé S., Alonso B., Durand J. O., Bujoli B., Gan Z.
762 and Hoatson G. (2002) Modelling one and two-dimensional solid-state NMR spectra. *Magn. Reson.*
763 *Chem.* **40**, 70–76.

McCammon, C.A., Pring, A., Keppler, H. and Sharp, T. (1995) A study of bernalite, Fe(OH)3, using Mössbauer spectroscopy, optical spectroscopy and transmission electron microscopy. *Phys. Chem. Miner*. **22**, 11–20.

McDowell, S.D, and Elders, W.A. (1980) Authigenic layer silicate minerals in borehole Elmoie l, Salton Sea geothermal field, California, *U.S.A Contrib. Miner. Petr.* **74**, 293-310.

Meunier, A. and Beaufort, D. (1996) Clay minerals in hydrothermal systems. *Geochim. Brasil.* **10**, 347-363.

Meunier, A. and Velde, B. (1989) Solid solution in I/S mixed-layer minerals and illite. *Amer. Miner.* **74**, 1106-1112.

Olives, J., Amouric, M. and Perbost, R. (2000) Mixed layering of illite-smectite: results from high-resolution transmission electron microscopy and lattice-energy calculations. *Clays Clay Miner.* **48**, 282-289.

Osborne, M.J. and Swarbrick, R.E. (1997). Mechanisms for generating overpressure in sedimentary basins: a reevaluation. *A.A.P.G. Bull*. **81**, 1023-1041.

Parkhurst, D.L. and Appelo, C. (2013). Description of input and examples for PHREEQC version 3—a computer program for speciation, batch-reaction, one-dimensional transport, and inverse geochemical calculations. *US geological survey techniques and methods*, book 6, 497.

Perbost, R., Olives, J. and Amouric, M. (2002) Thermodynamic stability of mixed-layer illite-smectite: Energetic calculations and microcalorimetric measurements, in: Hoteit, S., Tijani & Shao (Ed.), Hydromechanical and Thermohydromechanical Behaviour of Deep Argillaceous Rock. Swets & Zeitlinger, Lisse, 77-88.

Perry, E. and Hower, J. (1970) Burial diagenesis in Gulf Coast pelitic sediments. *Clays Clay Miner.* **18**, 265-274.

787 Powers, M.C. (1967). Fluid-release mechanisms in compacting marine mudrocks and their
788 importance in oil exploration. *A.A.P.G. Bull*. **51**, 1240-1254.

789 Steiner, A. (1968) Clay minerals in hydrothermally altered rocks at Wairakei, New Zealand. Clays
790 Clay Miner. **16**, 193-213.

791 Savage, D. (2011). A review of analogues of alkaline alteration with regard to long-term barrier
792 performance. *Mineralogical Magazine* **75**, 2401-2418.

793 Savage, D., Walker, C., Arthur, R., Rochelle, C., Oda, C. and Takase, H. (2007). Alteration of
794 bentonite by hyperalkaline fluids: A review of the role of secondary minerals. *Phys. Chem. Earth*,
795 Parts A/B/C **32**, 287-297.

796 Srodon J. and Eberl, D. (1984) Illite: in *Micas, Reviews in Mineralogy, **13**,* S. W. Bailey, ed.,
797 Mineralogical Society of America, Washington, *D.C.,* 495-544.

798 Townsend M.G., Longworth G. and Kodama H. (1986) Magnetic interaction at low temperature in
799 chlorite and its products of oxidation: a Mössbauer investigation. *Can. Miner.* **24**, 105-115.

800 Ulbrich H.H. and Waldbaum D.R. (1976) Structural and other contributions to the third-law entropies
801 of silicates. *Geochim. Cosmochim. Acta* **40**, 1–24.

802 Velde, B. and Vasseur, G. (1992) Estimation of the diagenetic smectite to illite transformation in
803 time-temperature space. *Amer. Miner.* **77**, 967-976.

804 Vieillard, P., Ramírez, S., Bouchet, A., Cassagnabère, A., Meunier, A. and Jacquot, E. (2004).
805 Alteration of the Callovo-Oxfordian clay from Meuse-Haute Marne Underground Laboratory (France)
806 by alkaline solution: II. Modelling of mineral reactions. *App. Geochem*. **19**, 1699-1709.

807 Watson, C., Hane, K., Savage, D., Benbow, S., Cuevas, J. and Fernandez, R. (2009). Reaction and
808 diffusion of cementitious water in bentonite: Results of 'blind' modelling. *App. Clay Sci.* **45**, 54-69.
809